Preparation, crystal structure and characterization of α-$NaSbP_2S_6$ and β-$NaSbP_2S_6$ phases

V. Manríquez *, A. Galdámez, D. Ruiz-León

Universidad de Chile, Facultad de Ciencias, Departamento de Química, Casilla 653, Santiago, Chile

Abstract

The new phases α-$NaSbP_2S_6$ and β-$NaSbP_2S_6$ were synthesized by ceramic and reactive flux methods at 773 K. The structures of α-$NaSbP_2S_6$ and β-$NaSbP_2S_6$ were determined by the single-crystal X-ray diffraction technique. α-$NaSbP_2S_6$ crystallizes in the monoclinic space group $P2_1/c$ with $a = 11.231(2)$ Å, $b = 7.2807(15)$ Å, $c = 11.640(2)$ Å, $\beta = 108.99(3)^\circ$, $V = 900.0(3)$ Å^3 and $z = 4$. β-$NaSbP_2S_6$ crystallizes in the monoclinic space group $P2_1$ with $a = 6.6167(13)$ Å, $b = 7.3993(15)$ Å, $c = 9.895(2)$ Å, $\beta = 92.12(3)^\circ$, $V = 484.10(17)$ Å^3 and $z = 2$.

The α- and β-phases of $NaSbP_2S_6$ are closely related, the main difference lies in the stacking of the $[Sb[P_2S_6]]_n^{n-}$ layers. The structure of α-$NaSbP_2S_6$ consists of two condensed layers (MPS_3 type) to give an ABAB... sequence with Na^+ cations located in the interlayer space. The packing of β-$NaSbP_2S_6$ is formed by monolayers of $[Sb[P_2S_6]]_n^{n-}$ stacked in an AA... fashion separated by a layer of Na^+ cations. Both phases are derivates of the $M^{1+}M^{3+}P_2Q_6$ family.

The optical band gaps of α-$NaSbP_2S_6$ and β-$NaSbP_2S_6$ were determined by UV–vis diffuse reflectance measurements to be 2.17 and 2.25 eV, respectively.

Keywords: A. Chalcogenides; B. Chemical synthesis; C. X-ray diffraction; D. Optical properties

1. Introductión

Many quaternary metal chalcophosphates $MM'[P_2Q_6]$ (Q = S, Se) have been studied in the last decades [1] because of their interesting structural properties as well as their potential technological importance as cathode materials for secondary batteries [2], non-linear optics [3] and photovoltaic devices [4,5]. On the other hand, the interest to prepare new materials of type $MM'[P_2Q_6]$ is due to the special coordination arrangement of the cations that determines structural characteristics and some physical properties.

The first reported quaternary chalcophosphates containing Bi and Sb were $A_3M(PS_4)_2$ (A = K, Rb, Cs; M = Sb, Bi); $Cs_3Bi_2(PS_4)_3$; $Na_{0.16}Bi_{1.28}P_2S_6$ [6]; $Cs_8M_4(P_2Se_6)_5$ [7] and KMP_2Q_6 (M = Bi, Sb; Q = S, Se) [8–11]. An important characteristic of the Bi and Sb atoms, in solid phases, is the stereochemical localization of the ns^2 electron pairs, which produces important variations in crystal structure, physical properties and electronic structure of the resulting materials. Thus, the structural diversity of quaternary chalcophosphates ranges from one dimensional chains of

* Corresponding author. Tel.: +56 2 9787388; fax: +56 2 2713888.
E-mail address: vmanriqu@uchile.cl (V. Manríquez).

Table 1
Crystal data and structure refinement for α-$NaSbP_2S_6$ and β-$NaSbP_2S_6$

Compound	α-$NaSbP_2S_6$	β-$NaSbP_2S_6$
Color and habit	Orange-yellow block	Orange-yellow block
Crystal size	0.08 mm × 0.07 mm × 0.04 mm	0.1 mm × 0.04 mm × 0.03 mm
Space group, z	$P2_1/c$, 4	$P2_1$, 2
a (Å)	11.231(2)	6.6167(13)
b (Å)	7.2807(15)	7.3993(15)
c (Å)	11.640(2)	9.895(2)
β (°)	108.99(3)	92.12(3)
V (Å^3)	900.0(3)	484.10(17)
μ (mm^{-1})	4.777	4.440
$2\theta_{max}$ (°)	28.05	28.04
$N(hkl)_{measured}$	7267 [R_{int} = 0.0354]	3826 [R_{int} = 0.0387]
$N(hkl)_{unique}$	2027	1952
$I_{obs} > 2\sigma(I_{obs})$	1757	1716
$N(param)_{refined}$	91	92
GooF (S)[a]	1.041	1.004
R1[b]	0.0369	0.0601
wR2[c]	0.0791	0.1463

[a]
[b] GooF $= \sqrt{\sum[w(F_o^2 - F_c^2)^2/(n-p)]}$.
[c] R1 $= \Sigma||F_o| - |F_c||/\Sigma|F_o|$.
wR2 $= \sqrt{\sum(w(F_o^2 - F_c^2)^2)/\sum w(F_o^2)^2}$.

Table 2
Fractional atomic coordinates and isotropic thermal parameter of α-$NaSbP_2S_6$

Átom	x	y	z	U_{eq}[a]
Sb	0.12994(3)	0.15937(4)	0.82053(3)	0.02273(12)
Na	0.4028(2)	0.6108(3)	0.1209(2)	0.0395(6)
P1	0.24686(11)	0.62251(16)	0.79604(11)	0.0148(3)
P2	0.24503(12)	0.40109(16)	0.66514(11)	0.0154(3)
S1	0.12637(12)	0.80910(16)	0.69172(11)	0.0197(3)
S2	0.06312(11)	0.30895(16)	0.60702(11)	0.0193(3)
S3	0.17414(12)	0.49255(16)	0.91597(11)	0.0201(3)
S4	0.34177(12)	0.19457(16)	0.77779(11)	0.0195(3)
S5	0.42267(12)	0.71019(17)	0.86842(12)	0.0220(3)
S6	0.31648(13)	0.49626(17)	0.54283(11)	0.0223(3)

[a] Equivalent isotropic U_{eq} defined as one third of the trace of the orthogonalized U_{ij} tensor.

Table 3
Fractional atomic coordinates and isotropic thermal parameter of β-$NaSbP_2S_6$

Átom	x	y	z	U_{eq}[a]
Sb	0.20605(10)	0.21940(13)	0.02000(7)	0.0168(3)
Na	0.3006(8)	0.9706(8)	0.4990(5)	0.0238(11)
P1	0.3118(7)	0.6774(6)	0.1747(5)	0.0431(13)
P2	0.2041(7)	0.4511(7)	0.2997(5)	0.0429(11)
S1	0.3412(8)	0.5644(7)	0.9864(5)	0.0483(11)
S2	0.0880(8)	0.8667(6)	0.1753(5)	0.0462(11)
S3	0.5741(7)	0.7656(6)	0.2552(5)	0.0462(12)
S4	0.9491(7)	0.3683(6)	0.1917(5)	0.0461(11)
S5	0.4177(8)	0.2588(7)	0.2689(5)	0.0525(14)
S6	0.1781(8)	0.5310(8)	0.4881(5)	0.0531(13)

[a] Equivalent isotropic U_{eq} defined as one third of the trace of the orthogonalized U_{ij} tensor.

Table 4
Selected bond distances (Å) and bond angles (°)

α-$NaSbP_2S_6$	
Sb1–S2	2.5909(14)
Sb1–S4	2.5967(14)
Sb1–S3	2.6469(13)
Sb1–S6	2.9733(16)
Sb1–S1	2.9523(12)
Sb1–S1[a]	3.0384(15)
P1–P2	2.2138(17)
S1–P1	2.0203(18)
S3–P1	2.0622(17)
S5–P1	1.9833(18)
S2–P2	2.0451(18)
S4–P2	2.0576(18)
S6–P2	1.9734(18)
S2–Sb1–S4	76.83(5)
S4–Sb1–S6	76.96(4)
S4–Sb1–S1	76.45(3)
S5–P1–S1	114.73(8)
S5–P1–S3	114.77(8)
S1–P1–S3	112.34(8)
S6–P2–S2	118.26(8)
S6–P2–S4	117.52(8)
S2–P2–S4	103.57(8)
β-$NaSbP_2S_6$	
Sb–S4	2.684(5)
Sb–S1	2.729(5)
Sb–S5	2.803(5)
Sb–S2	2.903(5)
Sb–S2[a]	3.142(5)
Sb–S3	3.153(5)
P1–P2	2.215(7)
P1–S3	1.993(6)
P1–S2	2.038(6)
P1–S1	2.058(7)
P2–S6	1.969(7)
P2–S5	2.036(7)
P2–S4	2.057(7)
S4–Sb–S1	84.91(15)
S4–Sb–S5	73.07(14)
S4–Sb–S2	80.94(15)
S3–P1–S2	113.3(3)
S3–P1–S1	112.6(3)
S2–P1–S1	112.0(3)
S6–P2–S5	115.9(3)
S6–P2–S4	118.8(3)
S5–P2–S4	106.0(3)

[a] Sb distance to S1 of the neighboring asymmetric units.

$A_3M(PS_4)_2$ (A = K, Rb, Cs; M = Sb, Bi), two-dimensional layered compounds $Cs_3Bi_2(PS_4)_3$ and KMP_2Q_6 (M = Bi, Sb; Q = S, Se) to the three-dimensional framework of $Na_{0.16}Bi_{1.28}P_2S_6$.

We have previously reported the crystal structures of the phases KMP_2S_6 (M = Bi, Sb), which are structurally related to $Fe_2P_2S_6$ [10,11]. In this work, we report the synthesis, crystal structure and optical properties of the new phases α-$NaSbP_2S_6$ and β-$NaSbP_2S_6$.

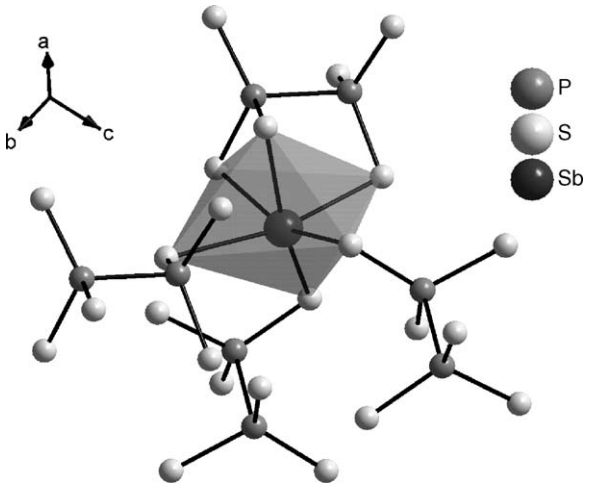

Fig. 1. Coordination of Sb^{3+} cations.

2. Experimental section

2.1. Synthesis

The preparation of the phase α-$NaSbP_2S_6$ was carried out by direct combination, in stoichiometric amounts, of powders of the corresponding high purity elements (99.99%), supplied by Aldrich, with an excess of sulfur (−1 mass%) to avoid the formation of impurity. The synthesis of the phase β-$NaSbP_2S_6$ was carried out by direct combination of the pure Sb and Na_2S, P_2S_5 and excess of S in ratio molar (1:1:1:1), so that all of the metal reacted to give well-crystallized products.

The reaction mixtures of both phases were sealed in evacuated quartz ampoules, and heated at 773 K for 1 week. All manipulations were carried out under Ar atmosphere. The reacted mixtures were slowly cooled to room temperature at the rate of 6 K/h and washed with DMF to remove the P_yS_x and S. The reaction products were washed and dried with anhydrous ether.

2.2. Characterization

Orange-yellow block-like crystals of α-$NaSbP_2S_6$ and β-$NaSbP_2S_6$ with dimensions 0.08 mm × 0.07 mm × 0.04 mm and 0.1 mm × 0.04 mm × 0.03 mm, respectively, were mounted on glass fibers. Single-crystal X-ray

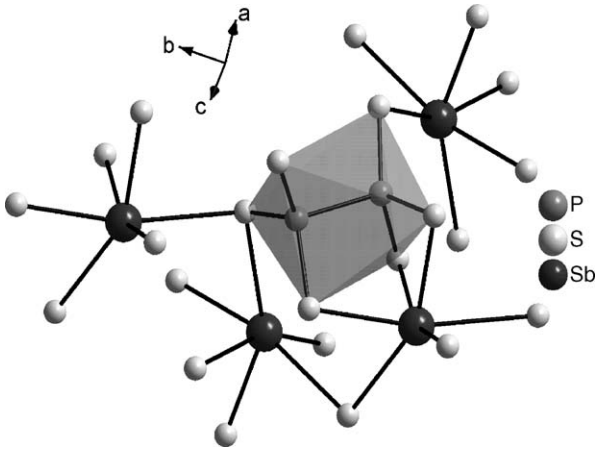

Fig. 2. Coordination of ethane-like anions $[P_2S_6]^{4-}$ ligands.

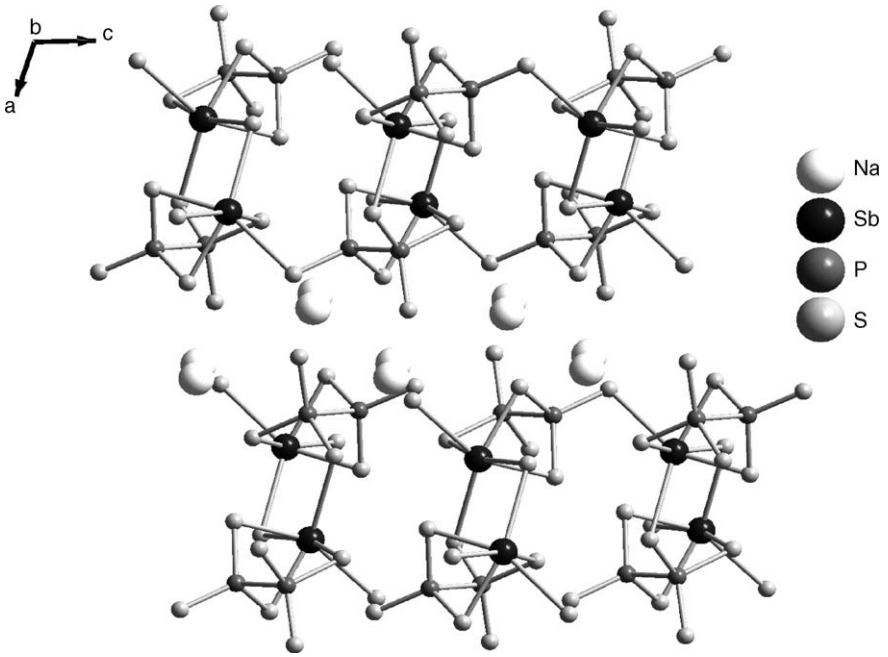

Fig. 3. Crystal structure of α-$NaSbP_2S_6$ viewed along *b*-axis.

diffraction data were obtained with the use of graphite-monochromatized Mo Kα radiation (λ = 0.71073 Å) at 293 K on a Bruker AXS SMART CCD area detector diffractometer. The collection of intensity data was carried out with the program SMART [12]. Cell refinement and data reduction were carried out with the program SAINT [12]. The empirical absorption correction was done using SADABS [12] and the structural solution (direct method) and all refinements were performed using the SHELXL package of crystallographic programs [13]. The systematic absences clearly pointed to the space groups $P2_1/c$ and $P2_1$ for α-$NaSbP_2S_6$ and β-$NaSbP_2S_6$, respectively. All atoms in both

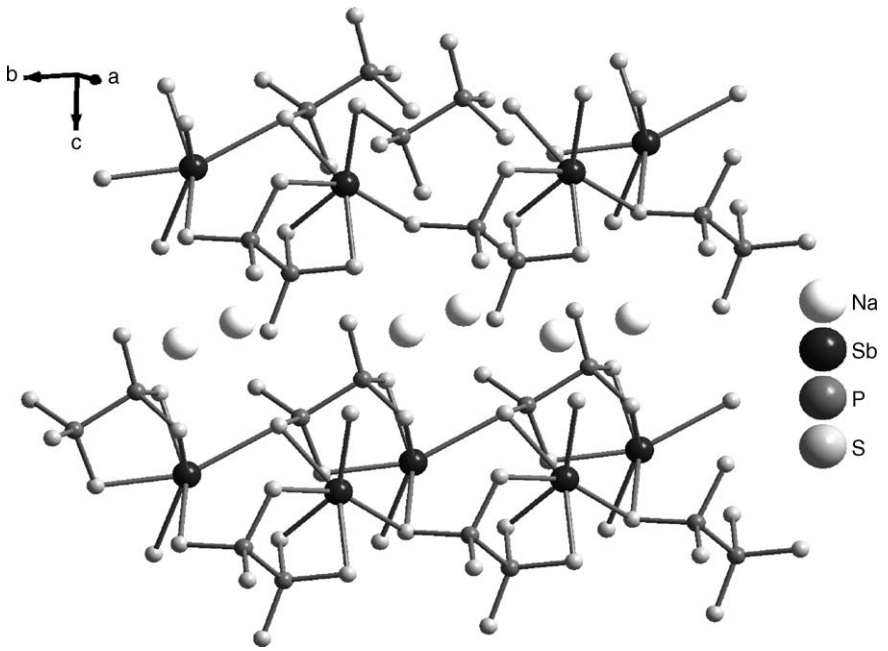

Fig. 4. Crystal structure of β-$NaSbP_2S_6$ viewed along *a*-axis.

phases were refined anisotropically to obtain final R1 and wR2 values 0.0369 and 0.0791; 0.0601 and 0.1463 for α- and β-phase, respectively. The maximum and minimum peaks on the final difference Fourier map corresponded to 1.497 and $-0.572\ e\text{Å}^{-3}$ for α-$NaSbP_2S_6$; 1.561 and $-1.044\ e\text{Å}^{-3}$ for β-$NaSbP_2S_6$. The crystal data are summarized in Table 1. The fractional atomic coordinates and equivalent isotropic thermal parameters are listed in Tables 2 and 3. Selected interatomic distances with their estimated standard deviation (esd's) are given in Table 4.

The diffuse reflectance UV–vis spectra were recorded using a UV-2450 SHIMADZU UV–visible spectrophotometer. $BaSO_4$ powder was used as reference at all energies (100% reflectance). Reflectance measurements were converted to absorption spectra using the Kubelka–Munk function.

3. Results and discussion

Both structures α,β-$NaSbP_2S_6$ are based upon a close packing of layered arrays of sulfur atoms. The sulfur atom stacking is $(ABC)_n$ for the α-phase and $(AB)_n$ for the β-phase. The layers are formed by ethane-like $[P_2S_6]^{4-}$ building blocks bridging the Sb atoms to form distorted octahedra. Thus, the structures can be described as layers of condensed S_6 distorted octahedra alternately centered by P_2 pairs and Sb atoms, which are held together by a single layer of Na^+ ions.

The distortion of the octahedron $[SbS_6]$ can partly be explained by the stereochemically active $5s^2$ lone pairs of Sb^{3+}. In accordance with the VSEPR model [15], lone pair bond repulsions in the antimony coordination sphere result in longer bond lengths for those bonds adjacent to the lone pair and shorter lengths for those more remote. Those repulsions give rise to an opening of the bond angles. The Sb^{3+} ions, in both phases, are tricoordinated by one ethane-like $[P_2S_6]^{4-}$ ligand and monocoordinated by three other $[P_2S_6]^{4-}$ groups forming chains (Fig. 1). One of those $[P_2S_6]^{4-}$ groups connects the Sb^{3+} to a neighboring chain, to form a layer in the *bc* plane. The bond lengths *d*(Sb–S) range for the α-phase from 2.5909(14) to 3.0384(15) Å and for the β-phase from 2.684(5) to 3.153(5) Å (Table 4). The *d*(Sb–S) are shorter than expected for a *d*(Sb–S) bond (4.03 Å) [16] and similar to that reported in $KSbP_2S_6$, Sb_2S_3 and Sb_2S_4 [10,17].

The ethane-like anion $[P_2S_6]^{4-}$ ligands chelate to four Sb atoms (Fig. 2); the bond lengths *d*(P–P) are 2.2138(17) Å for α-$NaSbP_2S_6$ and 2.215 (7) Å for β-$NaSbP_2S_6$. The bond lengths *d*(P–S) range from 1.9734(19) to 2.0622(17) Å in

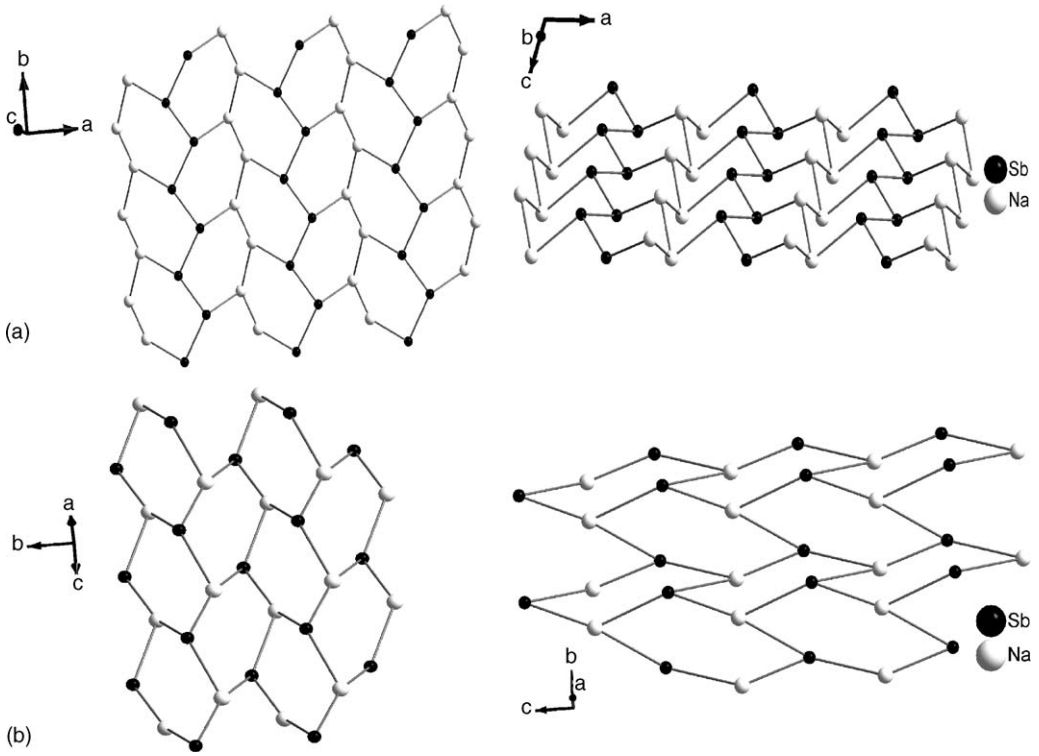

Fig. 5. Arrangement of cations in one layer and the corresponding side view: (a) α-$NaSbP_2S_6$ and (b) β-$NaSbP_2S_6$.

α-$NaSbP_2S_6$ and from 1.969(7) to 2.057(7) Å in β-$NaSbP_2S_6$ (Table 4). The bond lengths *d*(P–P) and *d*(P–S) are very similar to those observed in $Na_{0.16}Bi_{1.28}P_2S_6$ [6], $NaMP_2S_6$ (M = Yb, Sm) [18], $KSbP_2S_6$ [10] and $Fe_2P_2S_6$ [19].

The α- and β-phases of $NaSbP_2S_6$ are closely related; the main difference lies in the stacking of the $[SbP_2S_6]_n^{n-}$ layers. The crystal structure of α-$NaSbP_2S_6$ consists of two layers of MPS_3 type condensed to a bilayered structure, to give an ABAB. . . sequence and separated by the Na^+ cations (Fig. 3). The Na^+ cations are not located in the middle of the interlayer space, but instead are nestled into holes present in the layers. The packing of the β-$NaSbP_2S_6$ is formed by monolayers of $[SbP_2S_6]_n^{n-}$ stacked in an AA. . . fashion. The $[SbP_2S_6]_n^{n-}$ layers in the *a*–*b* plane are held together by a single layer of Na^+ ions (Fig. 4). The Na–S distances range for the α-phase from 3.027(3) to 3.105(3) Å and for the β-phase from 3.206(8) to 3.353(8) Å. In the compounds Na_6MnS_4 [14] and $Na_{0.16}Bi_{1.28}P_2S_6$ [6], the corresponding Na–S distances range from 2.734(3) to 3.203(3) Å and 2.839(3) to 3.190(4) Å, respectively.

In the quaternary metal thiophosphates $M^{1+}M^{3+}P_2S_6$, the postulated arrangements of the cations M^{1+} and M^{3+} in graphite-like configuration are triangular, zigzag and pairing of like atoms [18]. The monolayer of cations in α-$NaSbP_2S_6$ and β-$NaSbP_2S_6$ has a triangular pattern. The cation sublattice in the α-phase can be described as fused six-membered rings in chair conformation, while the β-phase presents alternate chains of six-membered rings in chair conformation (Fig. 5).

The optical properties of orange-yellow crystals of α-$NaSbP_2S_6$ and β-$NaSbP_2S_6$ were measured by UV–vis diffuse reflectance. The optical band gap corresponds to the intersection point between the base line along the energy axis and the extrapolated line from the linear portion of the threshold. The spectra confirm the semiconducting nature of the materials (Fig. 6). The optical band gaps of α-$NaSbP_2S_6$ and β-$NaSbP_2S_6$ are 2.17 and 2.25 eV, respectively. By comparison, the corresponding band gap of Sb_2S_3 is 1.7 eV [20].

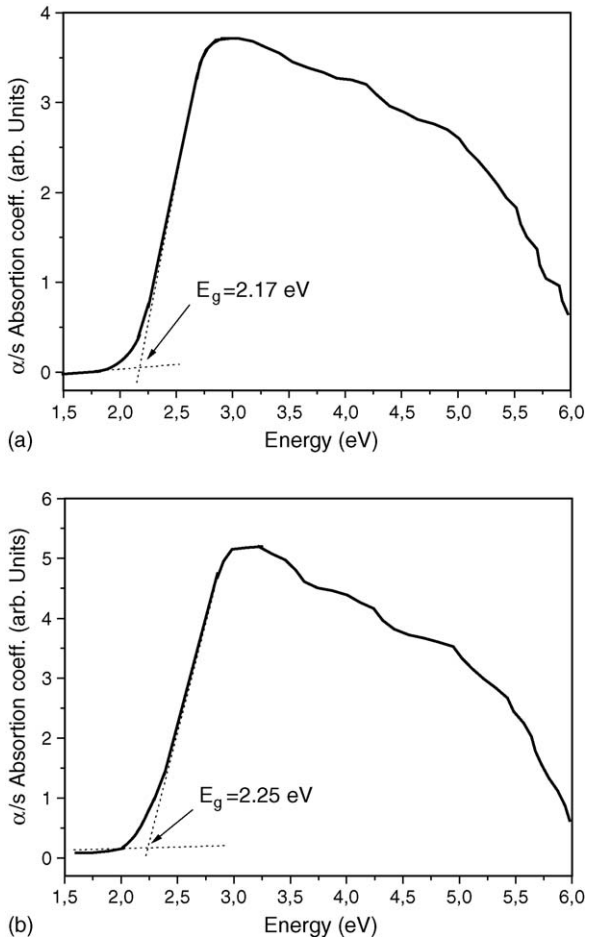

Fig. 6. The optical absorption spectrum of (a) α-$NaSbP_2S_6$ and (b) β-$NaSbP_2S_6$.

Acknowledgements

This work was supported by FONDECYT through operating grants No. 1020683. The authors thank the FONDAP No. 11980002 for the Bruker SMART CCD single-crystal diffractometer.

References

[1] M.G. Kanatzidis, Curr. Opin. Solid State Mater. Sci. 2 (1997) 139.
[2] (a) M.S. Whittingham, J. Electrochem. Soc. 123 (1976) 315;
(b) A.H. Thompsom, M.S. Whittingham, Mater. Res. Bull. 12 (1977) 741;
(c) M.S. Whittingham, A.J. Jacobson, Intercalation Chemistry, Academic Press Inc., New York, 1982, pp. 267–283.
[3] I. Lagadic, P.G. Lacroix, R. Clement, Chem. Mater. 9 (1997) 2004.
[4] M. Teman, A. Katty, C. Levy-Clement, P. Lemasson, Mater. Res. Bull. 17 (1982) 579.
[5] H.J. Moller, Semiconductor for Solar Cell, Artech House, Boston, 1993.
[6] T. McCarthy, M.G. Kanatzidis, J. Alloys Comp. 236 (1996) 70.
[7] T. McCarthy, T. Hogan, C. Kannewurf, M.G. Kanatzidis, Chem. Mater. 6 (1994) 1072.
[8] J. Breshears, M.G. Kanatzidis, J. Am. Chem. Soc. 122 (2000) 7839.
[9] J. Aitken, et al. Inorg. Chem. 38 (1999) 4795.
[10] V. Manríquez, A. Galdámez, D. Ruiz-León, M.T. Garland, Z. Krist, NCS 218 (2003) 403.
[11] V. Manríquez, A. Galdámez, D. Ruiz-León, M.T. Garland, M. Jiménez, Z. Krist, NCS 218 (2003) 1.
[12] SMART, SAINTPLUS V6.02, SHELXTL V6.10 and SADABS, Bruker Analytical X-ray Instruments Inc., Madison, WI, USA.
[13] G.M. Sheldrick, SHELXL-97. Program for the Refinement of Crystal Structures, University of Göttingen, Germany, 1997.
[14] W. Bronger, H. Balkhardtdegen, Z. Anorg. Allg. Chem. 574 (1989) 89.
[15] R.J. Gillespie, Can. J. Chem. 38 (1960) 818.
[16] R.D. Shannon, Acta Cryst. A 32 (1976) 751.
[17] F. Hulliger, Structural Chemistry of Layered-Type phases, D. Riedel Publishing Company, Dordrecht, Holland/Boston, USA, 1976pp. 62–77.
[18] E.-Y. Goh, E.-J. Kim, S.-J. Kim, J. Solid State Chem. 160 (2001) 195.
[19] W. Klingen, G. Eulenberger, H. Hahn, Z. Anorg, Allg. Chem. 401 (1973) 97.
[20] R.H. Bube, Photoconductivity of Solids, John Wiley and Sons Inc., New York, 1960, pp. 233–234.